"Heavy Electron" Photoelectron Spectroscopy: Rotationally Resolved Ion Pair Imaging of CH_3^+

Xianghong Liu, Richard L. Gross, Arthur G. Suits*

We applied the velocity map imaging technique under high-resolution conditions to study ion pair products of the vacuum ultraviolet photodissociation of methyl chloride. We obtained rotationally resolved kinetic energy release spectra that directly provide vibrational frequencies and rotational constants of the fundamental carbocation, CH_3^+. The technique is analogous to photoelectron spectroscopy, with the chloride anion playing the role of a "heavy electron." The approach shows promise as a general probe of ionic species not amenable to study by traditional methods.

The methyl cation is found in discharges, in mass spectrometry, and in interstellar clouds, and its properties are important in such diverse areas as chemical kinetics, combustion, quantum chemistry, plasma physics, and astrochemistry. Despite its broad importance and fundamental nature, the experimental challenges associated with the study of its spectroscopy have prevented general insight into the properties of this molecule. Indeed, the same challenges are generally faced by spectroscopists interested in determining the properties of a variety of fundamental ions. Photoelectron spectroscopy (PES), for example, is a powerful and nearly universal tool (*1*), but there are a great number of systems for which it is not applicable, because of the absence of suitable neutral molecules as precursors or because of the presence of large differences in geometry between the neutral and the ion that prevent access to the lowest levels of the ion. Even with direct probe techniques such as infrared absorption, the absence of laser sources in some regions, unaccommodating selection rules, and the difficulty of generating ions under well-defined conditions often make broad spectroscopic studies difficult or intractable. As a result, there is little or no experimental data on many fundamental systems (*2*, *3*). The nonclassical carbonium ions such as CH_5^+ and its homologs and protonated water and its clusters are important examples beyond the methyl cation.

The use of photoinduced threshold ion pair production (TIPPS) (*4*, *5*) has recently emerged as an extremely accurate means of probing ion energetics. Unfortunately, this approach has limitations that have so far prevented its application to polyatomic molecules. Inspired by the TIPPS work, we recently (*6*) reported application of the velocity map imaging technique (*7*, *8*) to study the photodissociation of molecules to ion pair products as a general means of probing ion energetics and spectroscopy. This approach, termed ion pair imaging ipectroscopy (IPIS), is fully analogous to PES but has the advantage that it may be applied to systems for which stable neutral precursors may not exist. In this case, the departing anion plays the role of a "heavy electron," and the result of ion pair dissociation of a stable molecule is to give the cation associated with ionization of a radical. This approach has the further advantage that it is a much slower process than photoelectron ejection, so that in principle larger regions of the cation configuration space may be accessed. A potential disadvantage is that the larger mass of the departing anion may produce a broad rotational distribution in the cation that could interfere with accurate determination of its spectroscopic properties. In this report, we show that IPIS can provide rotationally resolved spectra that completely eliminate the uncertainty introduced by the rotational broadening and instead allows determination of additional spectroscopic properties. Other groups have recently reported the use of ion pair imaging with single ion (*9*) and coincident ion pair detection (*10*), under low-resolution conditions, as a probe of photochemical dynamics in the vacuum ultraviolet (VUV).

The IPIS technique is illustrated schematically in Fig. 1 for the case of ion pair dissociation of CH_3Cl. Excitation in the VUV leads to a Rydberg state that couples to the long-range ion pair state. Dissociation of this state gives rise to momentum-matched Cl^- and CH_3^+ products, either of which may be detected with velocity map imaging. For a structureless atomic anion such as Cl^-, the kinetic energy release directly reflects the internal energy levels in the cation, just as in PES. For the CH_3Cl case, the kinematics are such that the results for the cation give significantly higher resolution, and there is no evidence of background interference from other sources of CH_3^+.

In a previous study, we applied the IPIS technique to this system under low-resolution conditions to demonstrate the method and to probe the ion pair dissociation dynamics of CH_3Cl at 118.3 nm. Here we applied the method under conditions of maximal velocity resolution to obtain a rotationally resolved and assigned spectrum for CH_3^+. The experimental apparatus has been described elsewhere (*11*). A beam of CH_3Cl seeded in H_2 (6%, at 3 atm backing pressure) was expanded from a piezoelectric pulsed valve and skimmed once before entering a main chamber. There it was crossed at 90° by a 118.2 nm VUV laser beam produced by frequency tripling the output of a Nd–yttrium-aluminum-garnet–pumped dye laser. The laser polarization was linear and was parallel to the detector plane. The ions were extracted along the beam axis (in contrast to our earlier experiment, in which the ions were extracted perpendicular to the beam) and focused by means of two-stage velocity mapping (*12*), directed through a field-free flight tube, and projected onto an 80-mm imaging detector. There were no grids anywhere in the

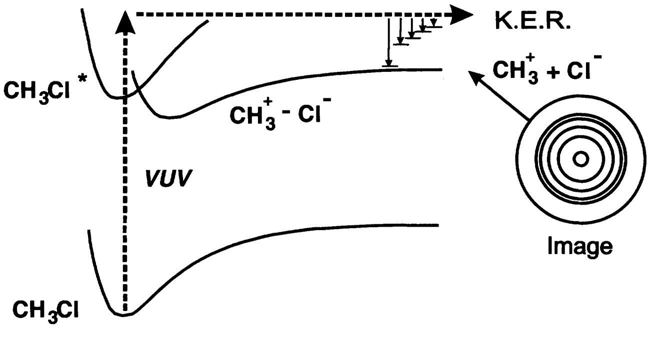

Fig. 1. Schematic representation of IPIS technique. K.E.R., kinetic energy release.

Gas Phase Molecular Dynamics Group, Chemistry Department, Brookhaven National Laboratory, Upton, NY 11973, USA, and Department of Chemistry, State University of New York at Stony Brook, Stony Brook, NY 11794–3400, USA.

*To whom correspondence should be adressed. E-mail: arthur.suits@sunysb.edu

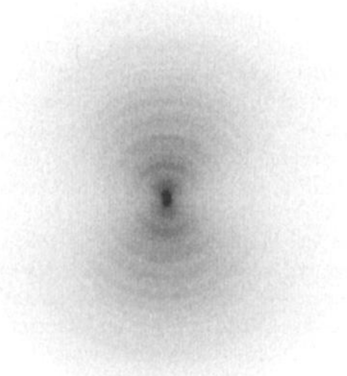

Fig. 2. Image of CH_3^+ from ion pair dissociation of methyl chloride at 118.2 nm. The laser polarization was vertical in the plane of the figure.

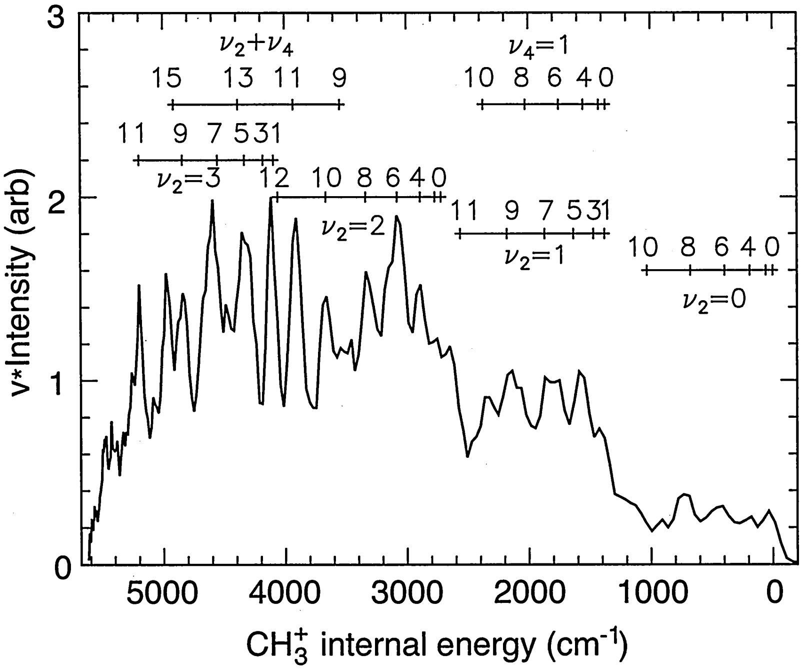

Fig. 3. IPIS spectrum for the ion pair process derived from the image in Fig. 2, shown with fitted rovibrational assignments. arb, arbitrary units.

Table 1. Comparison of calculated and experimental vibrational frequencies for CH_3^+ (in cm^{-1}). Uncertainties (in parentheses) are estimates based on sensitivity of the fits to a number of spectra.

Source	ν_1 (a_1')	ν_2 (a_2'')	ν_3 (e')	ν_4 (e')
MP2/aug-cc-pVTZ-*d*(H)-*f* (C)*	2912	1357	3108	1377
Experiment	–	1380 (20)†	3108.4‡	–
This work	–	1359 (7)	–	1370 (7)

*(*21*). †(*22*). ‡ (*23*).

ion flight path, and the front face of the detector was always held at ground potential. The detector was viewed by an integrating video system that accumulates images of the centroids of the ion spots as described elsewhere (*13*, *14*). Anion or cation images are readily obtained by reversing the voltages applied to the ion optics.

In a raw experimental image of CH_3^+ (Fig. 2), each of several rings represents single rovibrational levels of CH_3^+. Significant angular anisotropy is seen that is indicative of a prompt dissociation event and a parallel dissociation mechanism. Images for Cl^- give virtually identical results but with lower resolution; the analysis was thus performed on the CH_3^+ data.

We analyzed the image using an iterative reconstruction method (*15*) that, compared with conventional inversion methods, was found to give more reliable results for the higher energy products and was free of the centerline noise. The translational energy distribution shown in Fig. 3 is not multiplied by the (1/velocity) Jacobian that would normally accompany the transformation from velocity to energy; we omit this simply so that the weaker fast products may be more easily seen in the spectrum. In addition, we offset the total translational energy distribution by the available energy, so that it represents a CH_3^+ internal energy spectrum. It is shown along with combs indicating fitted rotational distributions for specific vibrational levels of CH_3^+. Despite care taken to maximize the velocity resolution in the experiment and to preserve the resolution through the inversion process, several factors work to undermine the ultimate resolution achievable under the present conditions. These include astigmatism in the ion optics, angular spread in the molecular beam, and noise in the inversion process; all of these factors may be improved in the future.

The fitting and assignment of the spectrum in Fig. 3 were accomplished as follows. The thermochemistry was taken from reference (*16*); the ionization potential of CH_3 was obtained from high-resolution pulsed-field ionization studies (*17*, *18*). Cooling of the parent CH_3Cl in the molecular beam gives rise to ortho ($K = 0$, where K is the projection of the total angular momentum J onto the principal axis) or para ($K = 1,2$) modifications that do not interconvert, and that were treated as two distinct populations. For the photodissociation event, we assume that K is conserved as a first approximation; this assumption has no effect on the subsequent analysis or assignments. The overall degeneracy and nuclear spin factors (*19*) are such that, for a given even value of ν_2 vibrational excitation (*20*), rotational levels with J even will have double the population compared to those with N odd, and for a given odd value of ν_2 vibrational excitation, rotational levels with N odd will have double the population compared to those with N even (*20*). This rule works greatly to our advantage in fitting the spectrum in Fig. 3, because alternate rotational levels have much lower population, and alternate levels in ν_2 excitation have contributions from different rotational levels with quite distinct spacing. The vibrational assignments for ν_2 versus ν_4 excitation may be made unambiguously via this distinct rotational spacing, even though the vibrational frequencies themselves are similar. Thus, we see the presence of both one quantum in ν_2 and one in ν_4 suggested by the rotational levels that appear in the vicinity of 2000 cm^{-1} in Fig. 3. Furthermore, in the vicinity of 4000 cm^{-1}, we see unambiguous evidence for excitation of a combination band with one quantum of ν_2 and one of ν_4, because an odd level ($N = 11$) appears with near equal intensity between peaks with two quanta in ν_2 and N even. This must be a peak with an odd number of quanta in ν_2, and the aforementioned combination band is the only possibility. This yields the first experimental measure of the ν_4 frequency, shown in Table 1. For the rotational constants, we have taken that for the vibrationless level from Oka's highly accurate high-resolution infrared studies (*21*, *22*), and all others were obtained by best fit of line spectra to the experimental data. Results for both observed vibrational

Table 2. Rotational constants (B) for specific vibrational levels of CH_3^+.

ν_2	ν_4	B (cm^{-1}) theory*	B (cm^{-1}) experiment
0	0	9.42	9.3623†
1	0	9.11	9.1
2	0	8.53	8.6
3	0	8.26	8.5
0	1	9.57	9.1
1	1	9.27	9.1

*(*24*). †(*23*).

frequencies are compared with previous experimental results and theoretical values in Table 1, and rotational constants for each vibrational level are presented in Table 2 and compared to theoretical results (*21*). Previous experimental values for vibrational frequencies have been reported only for the ν_2 (umbrella) (*22*) and ν_3 (C–H asymmetric stretch) modes (*23*, *24*), and there is considerable uncertainty in the former (see Table 1). A tentative assignment of ν_1 was made in our earlier low-resolution study, but it is apparent now that this was probably a single rotational line for $\nu_2 = 3$. Aside from Oka's value for the vibrationless level and the strongly allowed ν_3 fundamental, there have been no experimentally determined rotational constants for this system; we thus compare the rotational constants in Table 2 to theoretical calculations (*25*).

These results also provide insight into the dissociation dynamics of the process. The observed distribution principally shows evidence for a progression in umbrella-mode excitation, which may be readily understood by considering the change in the CH_3 geometry from the near-tetrahedral configuration of the parent molecule to the stiffly planar CH_3^+. In addition to the umbrella-mode progression, we also see evidence for some ν_4 excitation, both alone and in combination with one quanta of ν_2. Although not necessarily anticipated by a naïve view of the dynamics, it may be that coupling of the initially prepared Rydberg state to the ion pair state is favored by this in-plane bend excitation.

References and Notes

1. J. Berkowitz, *Photoabsorption, Photoionization and Photoelectron Spectroscopy* (Academic Press, New York, 1979).
2. E. Hirota, *Chem. Rev.* **92**, 141 (1992).
3. ———, *Annu. Rev. Prog. Chem. C* **96**, 95 (2000).
4. J. D. D. Martin, J. W. Hepburn, *Phys. Rev. Lett.* **79**, 3154 (1997).
5. ———, *J. Chem. Phys.* **109**, 8139 (1998).
6. M. Ahmed, D. S. Peterka, P. Regan, X. H. Liu, A. G. Suits, *Chem. Phys. Lett.* **339**, 203 (2001).
7. M. V. Frohne, thesis, Kansas State University, Manhattan, KS (1994).
8. A. Eppink, D. H. Parker, *Rev. Sci. Instrum.* **68**, 3477 (1997).
9. M. Kawasaki, K. Suto, Y. Sato, Y. Matsumi, R. Bersohn, *J. Phys. Chem.* **100**, 19853 (1996).
10. Y. Hikosaka, J. H. D. Eland, *Rapid Commun. Mass Spectrom.* **14**, 2305 (2000).
11. M. Ahmed, D. Blunt, D. Chen, A. G. Suits, *J. Chem. Phys.* **106**, 7617 (1997).
12. A low field ionization stage injects the ions into high field acceleration and focusing lenses, resulting in reduced aberration as compared to single-stage velocity mapping (X. Liu, R. L. Gross, A. G. Suits, unpublished results).
13. B. Y. Chang, R. C. Hoetzlein, J. A. Mueller, J. D. Geiser, P. L. Houston, *Rev. Sci. Instrum.* **69**, 1665 (1998).
14. W. M. Jackson, D. Xu, R. J. Price, K. L. McNesby, I. A. McLaren, in *Imaging in Chemical Dynamics*, A. G. Suits, R. E. Continetti, Eds. (American Chemical Society, Washington, DC, 2000), pp. 103–25.
15. M. J. J. Vrakking, *Rev. Sci. Instrum.* **72**, 4084 (2001).
16. L. V. Gurvich, I. V. Veyts, C. B. Alcock, *Thermodynamics Properties of Individual Substances* (Hemisphere, New York, 1989).
17. J. A. Blush, P. Chen, R. T. Wiedmann, M. G. White, *J. Chem. Phys.* **98**, 3557 (1993).
18. M. Litorja, B. Ruscic, *J. Chem. Phys.* **107**, 9852 (1997).
19. M. Zahedi, J. A. Harrison, J. W. Nibler, *J. Chem. Phys.* **100**, 4043 (1994).
20. The vibrational modes for CH_3^+ are ν_1, C-H symmetric stretch; ν_2, out-of-the-plane bend; ν_3, degenerate C-H stretch; ν_4, degenerate bend.
21. For the ortho forms, the nuclear spin factor g_{NK} = 0 and 4 for J odd and even, respectively, of vibrational levels with even quanta of ν_2 excitation. For odd quanta of ν_2 excitation, the situation is reversed, and only odd rotational levels are permitted. For the para modifications, this constraint is not present, and J odd or even may be equally populated.
22. R. V. Olkhov, S. A. Nizkorodov, O. Dopfer, *J. Chem. Phys.* **108**, 10046 (1998).
23. J. Dyke, N. Jonathan, E. Lee, A. Morris, *J. Chem. Soc. Faraday Trans. 2* **72**, 1385 (1976).
24. M. W. Crofton, W. A. Kreiner, M. F. Jagod, B. D. Rehfuss, T. Oka, *J. Chem. Phys.* **83**, 3702 (1985).
25. M. W. Crofton, M. F. Jagod, B. D. Rehfuss, W. A. Kreiner, T. Oka, *J. Chem. Phys.* **88**, 666 (1988).
26. W. P. Kraemer, V. Spirko, *J. Mol. Spec.* **149**, 235 (1991).

27. We thank G. Hall and T. Sears for valuable discussions. Supported by the Director, Office of Energy Research, Office of Basic Energy Sciences, Chemical Sciences Division, of the U.S. Department of Energy under contract DE-AC02-98CH1086.

26 September 2001; accepted 8 November 2001

Regional $^{14}CO_2$ Offsets in the Troposphere: Magnitude, Mechanisms, and Consequences

Bernd Kromer,[1]* Sturt W. Manning,[3] Peter Ian Kuniholm,[4] Maryanne W. Newton,[4] Marco Spurk,[5] Ingeborg Levin[2]

Radiocarbon dating methods typically assume that there are no significant tropospheric $^{14}CO_2$ gradients within the low- to mid-latitude zone of the Northern Hemisphere. Comparison of tree ring ^{14}C data from southern Germany and Anatolia supports this assumption in general but also documents episodes of significant short-term regional $^{14}CO_2$ offsets. We suggest that the offset is caused by an enhanced seasonal $^{14}CO_2$ cycle, with seasonally peaked flux of stratospheric ^{14}C into the troposphere during periods of low solar magnetic activity, coinciding with substantial atmospheric cooling. Short-term episodes of regional $^{14}CO_2$ offsets are important to palaeoclimate studies and to high-resolution archaeological dating.

The basic assumption about the atmospheric distribution of ^{14}C is that, although sources of ^{14}C-depleted C (such as outgassing of CO_2 from the ocean mixed layer) or ^{14}C-enriched C (such as intrusion of newly produced ^{14}C from the stratosphere) are restricted to certain areas and thus could leave a regional $^{14}CO_2$ imprint, rapid atmospheric mixing produces an efficient dispersion of $^{14}CO_2$ gradients. Hence, over even short time spans, on the order of 1 month, there are approximately uniform hemispheric levels of ^{14}C. In consequence, a cornerstone of ^{14}C dating is the assumption of a spatially uniform $^{14}CO_2$ source level during carbon uptake by plants, allowing us to provide and employ a single universal ^{14}C data set for the calibration of the ^{14}C time scale (*1*, *2*).

Support for the assumption that any regional $^{14}CO_2$ differences are small and may be ignored (that is, they are close to the detection limits of

---

[1]Heidelberger Akademie der Wissenschaften, [2]Institut für Umweltphysik der Universität Heidelberg, Im Neuenheimer Feld 229, D-69120 Heidelberg, Germany. [3]Department of Archaeology, University of Reading, Post Office Box 218 Whiteknights, Reading RG6 6AA, UK. [4]The Malcolm and Carolyn Wiener Laboratory for Aegean and Near Eastern Dendrochronology, B-48 Goldwin Smith Hall, Cornell University, Ithaca, NY 14853–3201, USA. [5]Institut für Botanik-210, Universität Hohenheim, D-70593 Stuttgart, Germany.

*To whom correspondence should be addressed. E-mail: bernd.kromer@iup.uni-heidelberg.de